

Affinity of C₆₀ Neat Fullerenes with Membrane Proteins: A Computational Study on Potassium Channels

Sebastian Kraszewski,[†] Mounir Tarek,^{‡,*} Werner Treptow,[§] and Christophe Ramseyer[†]

[†]Institut UTINAM, UMR 6213, CNRS Université de Franche, Comté, Besançon, France, [‡]UMR Structure et Réactivité des Systèmes Moléculaires Complexes, Nancy-University, CNRS, France, and [§]Laboratório de Biologia Teórica e Computacional, Universidade de Brasília, Brasil

ABSTRACT Most studies of the interactions of neat and functionalized fullerenes with cells have focused so far on their ability to cross the cell membrane envelopes. Membranes are, however, also host to a large number of proteins responsible for various cellular functions. Among these, ion channels are prominent components of the nervous system. Recently, it was shown that fullerenes may act as blockers or modulators of a variety of K⁺ channels. Here we use computer simulations to investigate the propensity of such nanocompounds to bind to K⁺ channels. Our results based on extensive atomistic molecular dynamics simulations reveal a variety of specific binding sites depending on the structure and properties of the channel. The corresponding binding free energies and putative mechanisms suggest that C₆₀ may indeed effectively hinder the function of K⁺ channels and hence induce toxicity.

KEYWORDS: fullerenes • ionic channels • toxicity • binding • molecular dynamics

The years to come will probably see a dramatic increase in the industrial generation and use of nanomaterials. Preliminary studies suggest that some types of nanoparticles might pose a health hazard, which could throw a shadow over the nanotech revolution. The impact of this development on worker safety, consumer protection, public health, and the environment has to be considered carefully, especially as the toxicity of nanomaterials is *a priori* not predictable from that of bulk material.^{1,2} Bulk carbon-based biomaterials have demonstrated excellent long-term biocompatibility and biological performances in medical device applications. This has thus led to many proposed applications for carbon-based nanostructures in the biomedical field, including biosensors and drug and vaccine delivery using carbon nanotubes (CNTs)^{3,4} and fullerenes (C₆₀).⁵ A lot of studies at the cellular level clearly suggest that fullerenes and, to a lesser extent, CNTs can cross the lipid membranes of cells.^{6–10} In addition, it was shown that functionalized CNTs are biocompatible with cells of the immune system (B and T lymphocytes as well as macrophages), indicat-

ing no apparent toxicity.¹¹ However, the cell membrane is not made of lipids only but also hosts a large amount of proteins that are responsible for the cell functions and activities.

Among them, K⁺ channels are responsible for nerve impulse by mediating conduction across synapses and, as such, are involved in a variety of biological processes, including cardiac, skeletal, and smooth muscle contraction, epithelial transport of nutrients and ions,¹² etc. K⁺ channels are complex quaternary structures in which the central hydrophilic pore results from an arrangement of four transmembrane (TM) domains. This pore domain is homologous to all K⁺ channels, and its structure has been first resolved for bacterial channels in the closed (KcsA)¹³ and open (MthK)¹⁴ states. The ionic pathway is delimited by the so-called selectivity filter (SF), a highly conserved sequence that allows these channels to discriminate K⁺ from other cations (see Supporting Information, Figure S1). K⁺ channels are a favorite target of several blockers and modulators such as toxins that inhibit, by a variety of mechanisms, their function.^{15–18} The so-called pore-blocking toxins^{19,20} and other small organic molecules, such as quaternary ammonium (QA) compounds, bind to the extracellular pore entryway of K⁺ channels and prevent ion conduction. Others permeate the channel from the intracellular side to reach binding sites inside the pore.^{21,22} In contrast, gating modifier peptides such as Hanatoxin and VSTX1 spider toxins^{16,23,24} are known to bind to voltage-gated potassium (Kv) channels. In these channels, the TM voltage sensing is ensured by a supplementary domain surrounding the pore, the so-called voltage sensor domain (VSD) that undergoes the

*Address correspondence to mtarek@edam.uhp-nancy.fr.

Received for review April 8, 2010 and accepted June 17, 2010.

Published online June 22, 2010.
10.1021/nn100723r

© 2010 American Chemical Society

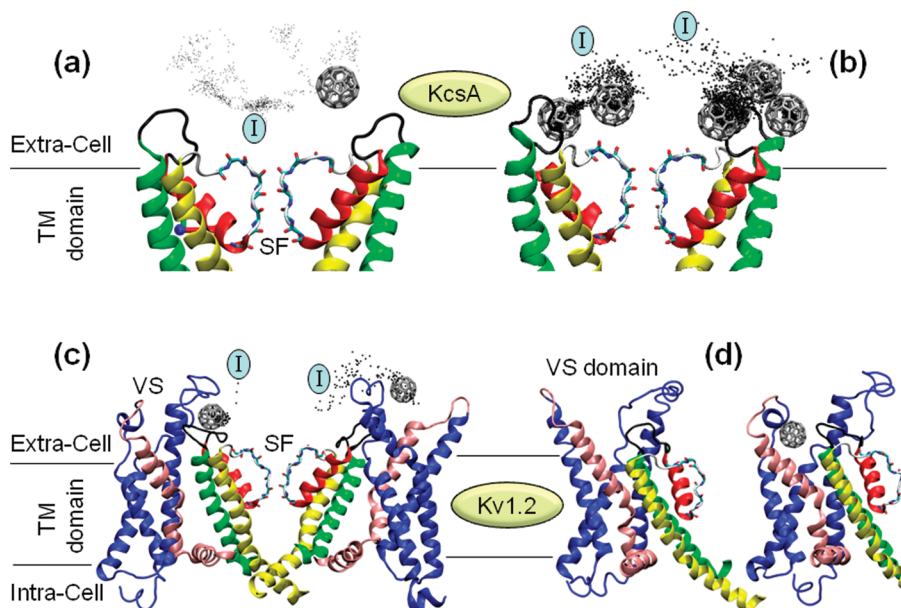


Figure 1. Binding of C_{60} to the extracellular domains of KcsA (top) and Kv1.2 (bottom). The dots represent the position of C_{60} along the MD trajectory sampled every 0.1 ns starting at position I and ending at the displayed C_{60} . Binding of (a) monomeric and (b) aggregates of C_{60} to the extracellular part of KcsA. (c) Binding of C_{60} to the voltage sensor domain (VSD) of Kv1.2. (d) Structure of the Kv1.2 VSD (d, left) before and (d, right) after binding of C_{60} . For clarity, the membrane lipids and the water molecules are not shown and only two monomers of each channel are displayed. KcsA channel is shown truncated in order to focus only on its extracellular side.

conformational changes necessary for opening of the intracellular gate.²⁵ The gating modifier toxins bind to this domain and alter the gating process by hindering its motion.

Owing to the complexity and diversity of K^+ channels, we investigate in this study the structural and energetic aspects of C_{60} binding mechanism to several channels, namely, KcsA, MthK, and Kv1.2. A preliminary study involving the use of *docking*-type calculations of C_{60} to KcsA and MthK channel revealed few binding sites and no affinity of fullerene to the ion channels' selectivity filter (see Supporting Information, Figure S2). These results clearly contrast with those of Park *et al.*,²⁶ who showed recently that C_{60} and single-walled carbon nanotubes (SWNTs) may act as blockers or modulators of K^+ channels expressed in mammalian CHO cells, while they have no effect on endogenous CHO cell CIC chloride channels.

As *docking* studies are of limited insight and are applied only to channel structures in vacuum, we have undertaken extensive MD simulations of the K^+ channels embedded in model membranes (see Methods section for more details) and interaction with mono- and oligomeric C_{60} molecules in order to shed light on the actions the latter may have on the channel's function.

RESULTS AND DISCUSSION

In contrast to the hypothesis put forward by Park *et al.*,²⁶ MD simulations of individual C_{60} molecules initially located near the extracellular mouth of the bacterial KcsA channel reveal no propensity of fullerenes to

bind to the SF (Figure 1a). However, monomeric C_{60} shows (within the 15 ns MD run) an affinity toward the hydrophobic residues of the extracellular loops linking segments S6 and the P helices. Control simulations considering six C_{60} placed near the SF evolved toward the same final conformation (Figure 1b) in which one C_{60} binds to the loops before aggregation of other C_{60} around the S6/P helix linker.

Hence, MD simulations indicate clearly that neither monomeric nor oligomeric C_{60} anchor to or block the SF of K^+ channels. The topology of the extracellular domain of voltage-gated K^+ (Kv) channels is far more complex than that of KcsA²⁷ (see Supporting Information, Figure S1) and provides for other binding sites. MD simulations of the mammalian Kv1.2 channel embedded in its membrane environment reveal indeed that C_{60} binds to the extracellular loops of the channel. All binding sites involve residues of the so-called voltage sensor domain (VSD). In some instances, C_{60} binds both to the VSD (in particular, the S1–S2 helices) and to S5–S6 (Figure 1c). In others, C_{60} binds specifically to the top of S3–S4 segments. Interestingly, in such a case, the VSD of the channel undergoes a large conformational movement "triggered" by the binding of C_{60} (Figure 1d).

In order to investigate the propensity of C_{60} molecules to bind to K^+ channels when approaching from the intracellular side, we have considered two scenarios. First, the MthK channel was used as a paradigm for open channel structures, and a fullerene molecule was placed in the intracellular membrane side, near the pore

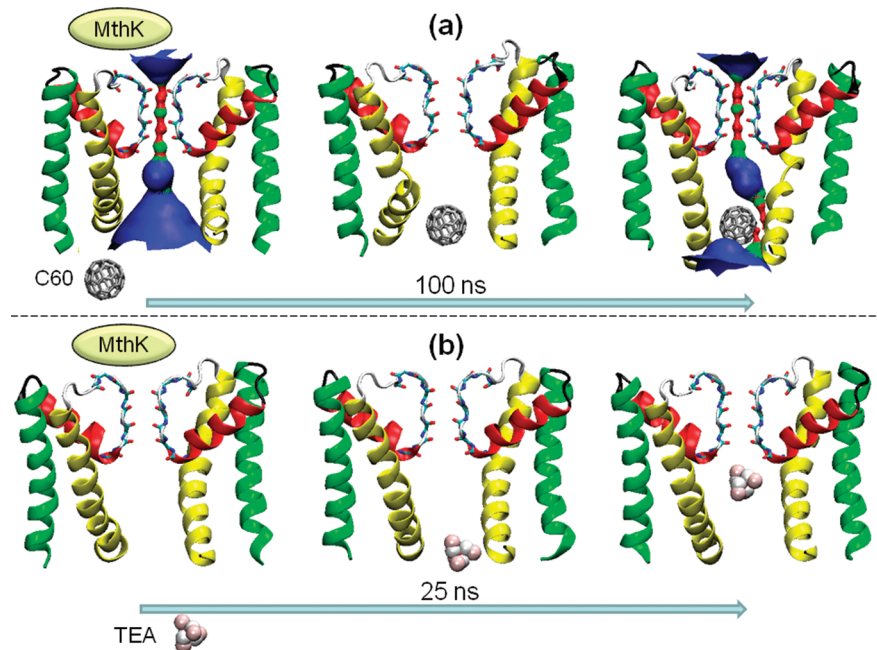


Figure 2. (a) Binding of C_{60} from the intracellular domain of MthK. From left to right: consecutive snapshots from MD simulations. The compound binds to the channel's gate and induces a blockage of the K^+ conduction pathway represented here (point density in color codes) by its hydrophilic pore volume.²⁸ (b) Snapshots from MD simulations of a tetraethylammonium (TEA) ion approaching the channel from the intracellular domain. Note that here TEA migrates through the channel gate toward its binding site inside the internal cavity.

entrance. During the simulation run (over 100 ns), the C_{60} migrates toward the internal cavity entrance (within 25 ns). Subsequently, a large conformational change of the M2 (S6) helices stabilizes the fullerene in its binding site (Figure 2a). This conformational change involves mainly a bending of the helix around the conserved glycine motif,¹⁴ favoring therefore interactions of the channel hydrophobic residues with the inclusion compound. Such a process bears a large resemblance to the concept of “hydrophobic seals” previously described for the KcsA channel²⁹ and causes a drastic alteration of the ion conduction pathway. To check whether the channel closing is correlated with the presence of C_{60} near the pore entrance, we performed a control simulation in which we considered tetraethylammonium (TEA), a widely used nonhydrophobic K^+ channel blocker.^{21,22} In agreement with experiments, when placed near the intracellular gate of MthK, TEA migrates through the gate to the central cavity toward its putative binding site³⁰ (Figure 2b). In contrast to the previous simulation, partial closing of the gate occurred only after TEA diffused toward the internal cavity.

Second, we investigated also the affinity of C_{60} to bind to the intracellular domain of Kv1.2. As in the MthK case, C_{60} molecules adequately placed near the gate bind quickly to the latter and “plug” the entrance of the channel (see Supporting Information, Figure S3).

Due to the hydrophobic character, C_{60} partitions in the membrane core^{7–9} and can therefore migrate laterally toward membrane proteins. MD simulations of C_{60} aggregates placed in the vicinity of a

model membrane show indeed, in agreement with previous experiments⁶ and simulations,^{7–9} that neat fullerenes partition toward the interior of the membrane (see Supporting Information, Figure S4). We have investigated using MD simulations the behavior of C_{60} placed in the lipid bilayer core and free to diffuse laterally toward MthK. While the approach to the channel, as expected, was diffusion driven, we sampled a trajectory in which a C_{60} reaches the channel and binds to a hydrophobic surface formed by an interhelical domain (Figure 3).

In summary, MD simulations of C_{60} show its propensity to interact with K^+ channels. The results point to a wide variety of locations that appear to be target sites of binding. In order to estimate the free energy of binding (BFE) associated with these sites, we have performed further calculations using the linear interaction energy (LIE) method.³¹ This approach allows a simple and efficient way³² of estimating the BFE from MD simulations of the ligand (here C_{60}) in associated and dissociated states (see Methods section and Supporting Information). Free energies of binding estimated with the LIE method may be not, for the present systems, as quantitatively reliable as those evaluated by other methods.

The BFE of C_{60} monomers and oligomers to the sites obtained from unconstrained simulations is reported in Table 1. For comparison, we report also results from simulations of TEA, the efficient K^+ channels blocker. Note that the latter binds strongly to the SF if approaching from the extracellular domain and to the

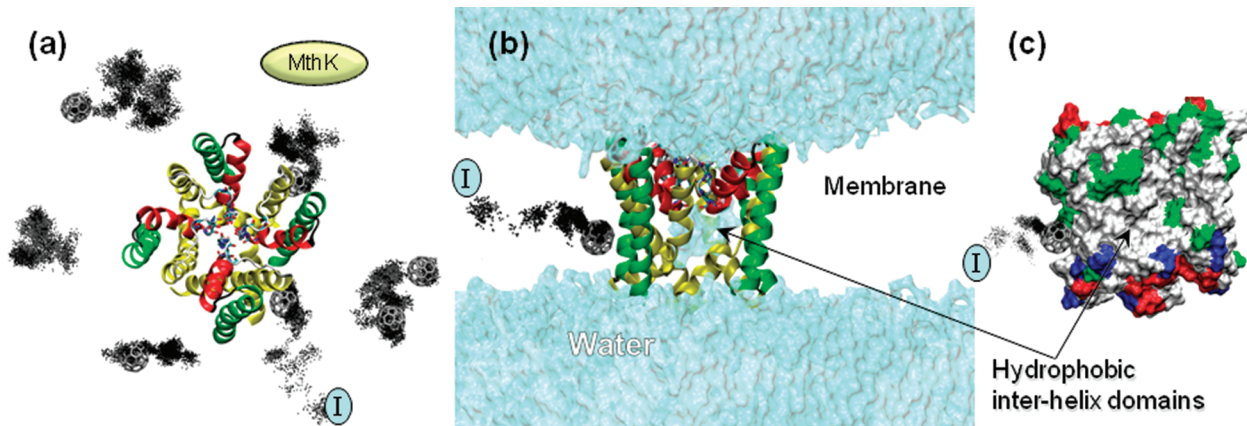


Figure 3. Binding of C_{60} to the transmembrane domain of MthK. (a) Top view. (b) Side view with a highlight of the solvent (blue) and the interhelices' binding domain; membrane not shown for clarity. (c) Same side view with a protein representation highlighting (white) the transmembrane hydrophobic protein domain. The dots represent the position of C_{60} along the MD trajectory sampled every 0.1 ns starting at position I and ending at the displayed C_{60} .

internal cavity when approaching from the intracellular domain. For all putative sites, the estimated BFEs of monomeric C_{60} are larger than ~ 2.4 kcal mol $^{-1}$ (*i.e.*, similar to the BFE of TEA to the SF of K^+ channels). The energies corresponding to the binding of fullerene to the MthK gate are somewhat larger probably due to its specific interaction with the M2 helices. The BFE of C_{60} to the extracellular domains of the voltage sensor of the Kv1.2 voltage-gated channel is also significant. This binding involves several channel amino acids that probably stabilize the protein– C_{60} complex. Finally, despite the affinity of C_{60} for the transmembrane domain of MthK, the free energy of partitioning between the hydrophobic membrane core and the channel is less than 1 kcal mol $^{-1}$. While the values of the estimated of C_{60} BFE from the present analysis ought to be taken with care, the comparison, under similar conditions with

binding of TEA, indicates that most of the putative target sites revealed by MD simulations involve a rather strong binding. In contrast to what has been suggested by Park *et al.*,²⁶ none of these sites corresponds to the mouth of the SF.

Despite the fact that C_{60} modulates ionic currents²⁶ and therefore the function of K^+ channels, the molecular mechanisms involved can only be inferred from comparison to the action of other blockers. When C_{60} binds to the intracellular pore domain, it is clear that it *plugs* the ionic conduction pathway. As for TEA,³³ we expect that such a block may be relieved by inward K^+ currents. The effect of binding to the VSD of Kv1.2 is less obvious. There is, however, a strong similarity to the binding of the gating modifier toxins. Such toxins bind to the top of S3 and S4 and shift the channel opening to more depolarized voltages.^{21,34} Compounds alike are believed to perturb the conformational freedom of the VSD, inhibiting directly the channel's activation. Given the large BFEs of C_{60} estimated from simulations and the structural effect it has on the VSD, our data suggest a similar scenario. Finally, partitioning of C_{60} in the membrane core allows accessibility to and binding to interhelical domains. This could hinder these helices' motion for several channels, altering therefore their function.

In summary, the results presented here provide an insight into the possible mechanisms governing the interaction of C_{60} with K^+ channels and a molecular view on their blockage capability. Further studies are needed in order to fully understand why C_{60} has no measurable effect on endogenous CHO cell CIC channels.²⁶ Two properties of the latter may be at the origin of the discrepancy. The CIC crystal structure³⁶ indicates indeed that (i) the mouth of the channel is lined with hydrophilic residues, which does not favor binding of C_{60} , and (ii) that the size of the hydrophilic ionic pathway is not large enough to allow

TABLE 1. Free Energies of C_{60} and TEA Binding to K^+ Channels (\pm Error Estimate)

protein	ligand	site	ΔG (kcal/mol)
KcsA	C_{60} (cluster of 2)	S6–P loop	-4.1 ± 0.7
	C_{60} (cluster of 4)	S6–P loop	-7.4 ± 1.0
	TEA	selectivity filter ^a	-2.4 ± 3.8^c
MthK	C_{60}	intracellular gate	-3.2 ± 0.4
	C_{60}	membrane side	-0.7 ± 0.4
	TEA	internal cavity ^b	-7.6 ± 4.0^d
Kv1.2	C_{60}	S1–S2/S5–S6	-3.3 ± 0.5
	C_{60}	S1–S2/S5–S6	-2.5 ± 0.5
	C_{60}	S3–S4	-3.0 ± 0.5
	C_{60}	intracellular gate	-1.9 ± 0.4

^aTEA bound in the conformation (TEA₀, W₁, K₂, W₃, K₄) of the SF, where W and K denotes a water molecule and potassium ion, respectively, and the subscripts relate to the specific sites of the SF; value averaged over 4 ns of simulation. ^bTEA bound in the conformation (K₁, W₂, K₃, W₄, TEA_{av}) of the SF; value averaged over last 5 ns of simulation. ^c(-4.0 ± 0.2) averaged over 200 ps of simulation from Luzhkov and Aqvist.³⁵ ^d(-4.2 ± 0.6) averaged over 200 ps of simulation from Luzhkov and Aqvist.³⁵

for diffusion of C_{60} inside the structure. Finally, binding of C_{60} to K^+ channels appears to depend mainly on the size and hydrophobicity of the compound, which holds for functionalized fullerenes. As the latter are potential

candidates for drug delivery,³⁷ our results suggest that, despite their suspected biocompatibility and low toxicity, their action on ion channels needs much further evaluation.

METHODS

Unconstrained full atomistic MD simulations were performed on three models of ionic channels belonging to potassium channel family. Considered channels were studied in a lipid environment composed of a hydrated palmitoyloleylphosphatidylcholine (POPC) lipid bilayer for MthK and Kv1.2 and a hydrated dioleylphosphatidylcholine (DOPC) lipid bilayer for KcsA. The binding sites of fullerene to different protein regions were first determined using docking and MD simulations and then confirmed by evaluation of the corresponding binding free energies (BFE) using the linear interaction energy (LIE) method.

Docking Method: In order to determine the channels' energetically favorable binding sites, the GRAMM (Global RAnge Molecular Matching) program³⁸ was used to dock C_{60} to KcsA and MthK channels structures (considered in vacuum). GRAMM is a fast-automated docking program that performs an exhaustive six-dimensional search through the relative intermolecular translations and rotations using a very efficient fast Fourier transform (FFT) correlation technique and a simple scoring function that measures shape complementarities and penalizes overlaps.

Two thousand docking solutions (poses) were computed and scored on a few different configurations for KcsA and MthK channels (see Supporting Information, Figure S2). Matching was performed in vacuum with minimal grid step of 1.4 Å for fullerenes. All interactions taken into account were based on included force field in generic mode, and the repulsion factor was equal to 30. The best complexes were chosen considering the best score of the docking results in which at least a ligand (C_{60}) molecule interacts with the internal or external part of the ion channel.

Fullerenes were found to bind preferentially at few extracellular sites and at few intracellular sites and showed no affinity for the selectivity filter. We have performed statistical analyses on the docking results. We have defined the binding constant as

$$K_P^{C_{60}}(l) = \frac{n_i \times E_{\text{score}}^{C_{60}}(i)}{\sum_{i=E,l} n_i \times E_{\text{score}}^{C_{60}}(i)}$$

which represents the statistical average of the score energy $E_{\text{score}}^{C_{60}}$ of the fullerene C_{60} over the docking simulations on the protein P. Here i denotes the two different potential locations of the C_{60} , namely, at the extracellular E or intracellular l side of the membrane.

For C_{60} , the two sites are statistically nearly equivalent for MthK since $K_{\text{MthK}}^{C_{60}}(E) = 0.48$ and $K_{\text{MthK}}^{C_{60}}(l) = 0.52$. For KcsA $K_{\text{KcsA}}^{C_{60}}(E) = 0.63$ and $K_{\text{KcsA}}^{C_{60}}(l) = 0.37$.

Molecular Dynamics Method: The MD simulations were performed using NAMD software.³⁹ They were conducted at a constant temperature of 300 K (Langevin dynamics) and a constant pressure of 1 atm using the Langevin piston Nosé–Hoover method.⁴⁰ Short- and long-range forces were calculated every 1 and 2 time steps, respectively, with a time step of 2.0 fs. Chemical bonds between hydrogen and heavy atoms were constrained to their equilibrium value. Long-range electrostatic forces were evaluated using the particle mesh Ewald (PME) method.⁴¹

The following molecular systems were studied. A summary of the MD simulation runs carried out is reported in Table 2 (total of 646 ns).

(i) **KcsA:** A three-dimensional model of KcsA (PDB code: 1bl8) was inserted at the center of a pre-equilibrated and fully hydrated DOPC lipid bilayer. The complete system (a total of ca. 90 300 atoms, $110 \times 106 \times 105 \text{ \AA}^3$) contains channel, 325 lipid molecules, 19 765 water molecules, and 10 chloride ions to ensure electroneutrality of the system. For more details see ref 27.

TABLE 2. MD runs carried out

molecular system	system description	total simulation time (ns)
(i)	KcsA in presence of monomeric C_{60}	15
(i)	KcsA in presence of six C_{60}	29
(ii)	MthK in presence of six C_{60} in the membrane and one C_{60} at the gate	119
(iii)	Kv1.2 in presence of four C_{60} in the solvent and one C_{60} at the gate	213
(iv)	four C_{60} in the vicinity of lipid membrane	101
(iv)	six C_{60} in a water box	60
(v)	KcsA in presence of TEA	10
(v)	MthK in presence of TEA	25

(ii) **MthK:** The open state K^+ MthK (PDB code: 1lnq) was embedded in a pre-equilibrated POPC bilayer. The total system contains the channel, 357 lipid molecules, 23 863 water molecules, and 10 sodium ions, that is, a total of ca. 103 500 atoms ($110 \times 109 \times 100 \text{ \AA}^3$).

(iii) **Kv1.2:** In this study, we considered only the TM domain (residues 122 to 390) of the voltage-gated channel Kv1.2⁴² (PDB code: 2a79) inserted at the center of a POPC membrane patch. The system contains 426 lipid molecules, 41 464 water molecules, and the 22 cations distributed in the solvent to ensure the electroneutrality of the system (a total of ca. 173 000 atoms, $130 \times 134 \times 110 \text{ \AA}^3$). More detailed information concerning equilibration process was described elsewhere,⁴³ and a general view on this system is provided in Supporting Information in Figure S5.

(iv) **C_{60} Fullerene:** The neat C_{60} carbon fullerene molecules were successively modeled with all systems containing ionic channels, in a water box or with fully hydrated POPC membrane patches. We investigated binding to the extracellular regions of K^+ channels using the KcsA channel model, binding to the intracellular open gate region and laterally through the hydrophobic transmembrane region using the opened MthK channel model, and binding to the voltage-gated channels using the Kv1.2 channel model.

(v) **Tetraethylammonium Ion (TEA):** A pyramidal configuration of one TEA ion was used to study binding to the extracellular side of the KcsA channel and binding to the intracellular open gate and internal cavity regions of the MthK channel.

(vi) **LIE Reference Systems:** The LIE method required supplementary simulations for each ligand (C_{60} or TEA) in a reference environment. Accordingly, the following molecular systems were also used: (a) one C_{60} molecule in a (48.5 \AA^3) water box; (b) aggregates of two and four C_{60} molecules in a water box; (c) one C_{60} molecule positioned in the hydrophobic region of a fully hydrated POPC lipid bilayer; (d) TEA in a water box. The simulations of the reference systems lasted 5 ns for each of the C_{60} systems and 54 ns for the TEA.

Linear Interaction Energy (LIE) Method: All systems were modeled using the CHARMM27⁴⁴ force field with a united atoms representation for the acyl chains of the lipid molecules. No charges were attributed to the C_{60} carbon atoms and for fullerene C–C or fullerene C–water oxygen interactions we used the Bedrov *et al.*⁴⁵ Lennard-Jones potential parameters (CHARMM27 functional: $\sigma_{CC} = 3.895 \text{ \AA}$, $\epsilon_{CC} = 0.066 \text{ kcal mol}^{-1}$, and $\sigma_{CO} = 3.58 \text{ \AA}$, $\epsilon_{CO} = 0.0936 \text{ kcal mol}^{-1}$). The potential parameters for TEA ion were taken from Crouzy *et al.*⁴⁶

For energetic properties analysis, we used the LIE method proposed by Aqvist *et al.* to study ionic channel blockage by qua-

ternary ammonium (QA) compounds such as TEA or by local anesthetics.^{32,35} The approach is based on the estimates of scaled differences between two MD simulations, one with the free ligand in its reference environment and one where the ligand bound to the protein. For all systems, the time evolutions of the binding energies are reported in Supporting Information.

The average free binding energies were computed as

$$\Delta G = \alpha \langle \langle V_{l-s}^{\text{vdW}} \rangle_{\text{bind}} - \langle V_{l-s}^{\text{vdW}} \rangle_{\text{free}} \rangle + \beta \langle \langle V_{l-s}^{\text{el}} \rangle_{\text{bind}} - \langle V_{l-s}^{\text{el}} \rangle_{\text{free}} \rangle$$

where ΔG is the Gibbs free energy of binding, V^{vdW} and V^{el} are the Lennard-Jones and the Coulomb ligand-surroundings potential interaction, respectively, the subscripts "free" and "bind" describe the ligand-free or the bound state, and α and β are empirical scaling factors. Following Luzhkov *et al.*, we used the scaling coefficients $\alpha = 0.18$ and $\beta = 0.52$.^{31,47} No electrostatic contribution was taken into account for fullerenes since their carbon atoms bear no partial charge.

Acknowledgment. This work was granted access to the HPC resources of the Centre Informatique National de l'Enseignement Supérieur (CINES) under the allocation 2009-075137 made by GENCI (Grand Equipment National de Calcul Intensif).

Supporting Information Available: Results of docking and MD calculations and details on the LIE method corresponding results. This material is available free of charge via the Internet at <http://pubs.acs.org>.

REFERENCES AND NOTES

1. Panessa-Warren, B. J.; Warren, J. B.; Wong, S. S.; Misewich, J. A. Biological Cellular Response to Carbon Nanoparticle Toxicity. *J. Phys.: Condens. Mater.* **2006**, *18*, S2185–S2201.
2. Smart, S. K.; Cassady, A. I.; Lu, G. Q.; Martin, D. J. The Biocompatibility of Carbon Nanotubes. *Carbon* **2006**, *44*, 1034–1047.
3. Ajayan, P. M. Nanotubes from Carbon. *Chem. Rev.* **1999**, *99*, 1787–1799.
4. Baughman, R. H.; Zakhidov, A. A.; de Heer, W. A. Carbon Nanotubes—The Route toward Applications. *Science* **2002**, *297*, 787–792.
5. Da Ros, T.; Prato, M. Medicinal Chemistry with Fullerenes and Fullerene Derivatives. *Chem. Commun.* **1999**, 663–669.
6. Sayes, C. M.; Fortner, J. D.; Guo, W.; Lyon, D.; Boyd, A. M.; Ausman, K. D.; Tao, Y. J.; Sitharaman, B.; Wilson, L. J.; Hughes, J. B.; *et al.* The Differential Cytotoxicity of Water-Soluble Fullerenes. *Nano Lett.* **2004**, *4*, 1881–1887.
7. Qiao, R.; Roberts, A. P.; Mount, A. S.; Klaine, S. J.; Ke, P. C. Translocation of C-60 and Its Derivatives across a Lipid Bilayer. *Nano Lett.* **2007**, *7*, 614–619.
8. Wong-Ekkabut, J.; Baoukina, S.; Triampo, W.; Tang, I. M.; Tielemans, D. P.; Monticelli, L. Computer Simulation Study of Fullerene Translocation through Lipid Membranes. *Nat. Nanotechnol.* **2008**, *3*, 363–368.
9. Bedrov, D.; Smith, G. D.; Davande, H.; Li, L. W. Passive Transport of C-60 Fullerenes through a Lipid Membrane: A Molecular Dynamics Simulation Study. *J. Phys. Chem. B* **2008**, *112*, 2078–2084.
10. Andreev, I.; Petrukhina, A.; Garmanova, A.; Babakhan, A.; Andreev, S.; Romanova, V.; Troshin, P.; Troshina, O.; DuBuske, L. Penetration of Fullerene C60 Derivatives through Biological Membranes. *Fullerenes, Nanotubes, Carbon Nanostruct.* **2008**, *16*, 89–102.
11. Bianco, A.; Prato, M. Can Carbon Nanotubes Be Considered Useful Tools for Biological Applications? *Adv. Mater.* **2003**, *15*, 1765–1768.
12. Hille, B. *Ionic Channels of Excitable Membranes*, 2nd ed.; Sinauer: Sunderland, MA, 1992.
13. Doyle, D. A.; Cabral, J. M.; Pfuetzner, R. A.; Kuo, A.; Gulbis, J. M.; Cohen, S. L.; Chait, B. T.; MacKinnon, R. The Structure of the Potassium Channel: Molecular Basis of K⁺ Conduction and Selectivity. *Science* **1998**, *280*, 69–77.
14. Jiang, Y.; Lee, A.; Chen, J.; Cadene, M.; Chalt, B. T.; MacKinnon, R. The Open Pore Conformation of Potassium Channels. *Nature* **2002**, *417*, 523–526.
15. Oseguera, A. J.; Islas, L. D.; Garcia-Villegas, R.; Rosenbaum, T. On the Mechanism of Tba Block of the Trpv1 Channel. *Biophys. J.* **2007**, *92*, 3901–3914.
16. Huang, P. T.; Shiao, Y. S.; Lou, K. L. The Interaction of Spider Gating Modifier Peptides with Voltage-Gated Potassium Channels. *Toxicon* **2007**, *49*, 285–292.
17. Yu, K. Q.; Fu, W.; Liu, H.; Luo, X. M.; Chen, K. X.; Ding, J. P.; Shen, J. H. Computational Simulations of Interactions of Scorpion Toxins with the Voltage-Gated Potassium Ion Channel. *Biophys. J.* **2004**, *86*, 3542–3555.
18. Holmgren, M.; Smith, P. L.; Yellen, G. Trapping of Organic Blockers by Closing of Voltage-Dependent K⁺ Channels—Evidence for a Trap Door Mechanism of Activation Gating. *J. Gen. Physiol.* **1997**, *109*, 527–535.
19. Ruta, V.; Jiang, Y. X.; Lee, A.; Chen, J. Y.; MacKinnon, R. Functional Analysis of an Archaeabacterial Voltage-Dependent K⁺ Channel. *Nature* **2003**, *422*, 180–185.
20. Eriksson, M. A. L.; Roux, B. Modeling the Structure of Agitoxin in Complex with the Shaker K⁺ Channel: A Computational Approach Based on Experimental Distance Restraints Extracted from Thermodynamic Mutant Cycles. *Biophys. J.* **2002**, *83*, 2595–2609.
21. Armstrong, C. M. Interaction of Tetraethylammonium Ion Derivatives with Potassium Channels of Giant Axons. *J. Gen. Physiol.* **1971**, *58*, 41.
22. French, R. J.; Shoukimas, J. J. Blockage of Squid Axon Potassium Conductance by Internal Tetra-N-alkylammonium Ions of Various Sizes. *Biophys. J.* **1981**, *34*, 271–291.
23. Lee, H. C.; Wang, J. M.; Swartz, K. J. Interaction between Extracellular Hanatoxin and the Resting Conformation of the Voltage-Sensor Paddle in Kv Channels. *Neuron* **2003**, *40*, 527–536.
24. Lee, S. Y.; MacKinnon, R. A Membrane-Access Mechanism of Ion Channel Inhibition by Voltage Sensor Toxins from Spider Venom. *Nature* **2004**, *430*, 232–235.
25. Yellen, G. The Voltage-Gated Potassium Channels and Their Relatives. *Nature* **2002**, *419*, 35–42.
26. Park, K. H.; Chhowalla, M.; Iqbal, Z.; Sesti, F. Single-Walled Carbon Nanotubes Are a New Class of Ion Channel Blockers. *J. Biol. Chem.* **2003**, *278*, 50212–50216.
27. Treptow, W.; Tarek, M. K⁺ Conduction in the Selectivity Filter of Potassium Channels Is Monitored by the Charge Distribution Along Their Sequence. *Biophys. J.* **2006**, *91*, L81–L83.
28. Smart, O. S.; Goodfellow, J. M.; Wallace, B. A. The Pore Dimensions of Gramicidin A. *Biophys. J.* **1993**, *72*, 1109–1126.
29. Kitaguchi, T.; Sukhareva, M.; Swartz, K. J. Stabilizing the Closed S6 Gate in the Shaker Kv Channel through Modification of a Hydrophobic Seal. *J. Gen. Physiol.* **2004**, *124*, 319–332.
30. Kutluay, E.; Roux, B.; Heginbotham, L. Rapid Intracellular Tea Block of the KcsA Potassium Channel. *Biophys. J.* **2005**, *88*, 1018–1029.
31. Aqvist, J.; Luzhkov, V. B.; Brandsdal, B. O. Ligand Binding Affinities from MD Simulations. *Acc. Chem. Res.* **2002**, *35*, 358–365.
32. Luzhkov, V. B.; Nilsson, J.; Arhem, P.; Aqvist, J. Computational Modelling of the Open-State K(V)1.5 Ion Channel Block by Bupivacaine. *BBA-Proteins Proteom.* **2003**, *1652*, 35–51.
33. Tagliafate, M.; Vandongen, A. M. J.; Drewe, J. A.; Joho, R. H.; Brown, A. M.; Kirsch, G. E. Patterns of Internal and External Tetraethylammonium Block in 4 Homologous K⁺-Channels. *Mol. Pharmacol.* **1991**, *40*, 299–307.
34. Swartz, K. J.; MacKinnon, R. Mapping the Receptor Site for Hanatoxin, a Gating Modifier of Voltage-Dependent Potassium Channels. *Neuron* **1997**, *18*, 675–682.
35. Luzhkov, V. B.; Aqvist, J. Mechanisms of Tetraethylammonium Ion Block in the KcsA Potassium Channel. *FEBS Lett.* **2001**, *495*, 191–196.

36. Dutzler, R.; Campbell, E. B.; Cadene, M.; Chait, B. T.; MacKinnon, R. X-ray Structure of a Cic Chloride Channel at 3.0 Angstrom Reveals the Molecular Basis of Anion Selectivity. *Nature* **2002**, *415*, 287–294.
37. Klumpp, C.; Lacerda, L.; Chaloin, O.; Da Ros, T.; Kostarelos, K.; Prato, M.; Bianco, A. Multifunctionalised Cationic Fullerene Adducts for Gene Transfer: Design, Synthesis and DNA Complexation. *Chem. Commun.* **2007**, *3762*–3764.
38. Vakser, I. A.; Matar, O. G.; Lam, C. F. A Systematic Study of Low-Resolution Recognition in Protein–Protein Complexes. *Proc. Natl. Acad. Sci. U.S.A.* **1999**, *96*, 8477–8482.
39. Phillips, J. C.; Braun, R.; Wang, W.; Gumbart, J.; Tajkhorshid, E.; Villa, E.; Chipot, C.; Skeel, R. D.; Kale, L.; Schulten, K. Scalable Molecular Dynamics with Namd. *J. Comput. Chem.* **2005**, *26*, 1781–1802.
40. Feller, S. E.; Zhang, Y. H.; Pastor, R. W.; Brooks, B. R. Constant-Pressure Molecular-Dynamics Simulation—The Langevin Piston Method. *J. Chem. Phys.* **1995**, *103*, 4613–4621.
41. Darden, T.; York, D.; Pedersen, L. Particle Mesh Ewald: An $N \cdot \log(N)$ Method for Ewald Sums in Large Systems. *J. Chem. Phys.* **1993**, *98*, 10089–10092.
42. Long, S. B.; Campbell, E. B.; MacKinnon, R. Crystal Structure of a Mammalian Voltage-Dependent Shaker Family K^+ Channel. *Science* **2005**, *309*, 897–903.
43. Treptow, W.; Tarek, M. Environment of the Gating Charges in the Kv1.2 Shaker Potassium Channel. *Biophys. J.* **2006**, *90*, L64–L66.
44. MacKerell, A. D.; Bashford, D.; Bellott, M.; Dunbrack, R. L.; Evanseck, J. D.; Field, M. J.; Fischer, S.; Gao, J.; Guo, H.; Ha, S.; et al. All-Atom Empirical Potential for Molecular Modeling and Dynamics Studies of Proteins. *J. Phys. Chem. B* **1998**, *102*, 3586–3616.
45. Li, L. W.; Bedrov, D.; Smith, G. D. Water-Induced Interactions between Carbon Nanoparticles. *J. Phys. Chem. B* **2006**, *110*, 10509–10513.
46. Crouzy, S.; Berneche, S.; Roux, B. Extracellular Blockade of K^+ Channels by Tea: Results from Molecular Dynamics Simulations of the KcsA Channel. *J. Gen. Physiol.* **2001**, *118*, 207–217.
47. Hansson, T.; Marelius, J.; Aqvist, J. Ligand Binding Affinity Prediction by Linear Interaction Energy Methods. *J. Comput.-Aided. Mol. Des.* **1998**, *12*, 27–35.